

## Electronic Supplementary Information

### Coupling of tyrosine deprotonation and axial ligand exchange in nitrocytochrome *c*

Daiana A. Capdevila, Damián Álvarez-Paggi, María A. Castro, Verónica Tórtora, Verónica Demicheli, Darío A. Estrín, Rafael Radi, Daniel H. Murgida

**Protein preparation and purification.** A large scale nitration and purification procedure was adapted from previously described methods.<sup>1,2</sup> Peroxynitrite was added as a continuous flow of 0.134 mM min<sup>-1</sup> during 20 min to Cyt (1 mM) under vigorous shaking in 200 mM potassium phosphate with 25 mM NaHCO<sub>3</sub> and 100 μM DTPA at pH 7.0 and 25°C. The final pH was always controlled and kept below 7.4.

After reaction, salts were removed by a chromatography step in a HiTrap desalting column (Amersham Biosciences) and the mixture of nitrated Cyt forms was passed through a cation exchange sulfopropyl-TSK preparative column (21.5 mm(ID) x 15.0 cm (L), Tosoh Biosep) in order to purify the mononitrated species<sup>1</sup>. The flow rate was 3 ml/min and the column was equilibrated with 5 mM ammonium acetate buffer (pH 9.0), kept during 5 min in this buffer and then peaks were eluted using a linear gradient from 5 mM to 150 mM ammonium acetate from 5 to 30 min, from 150 mM to 400 mM ammonium acetate from 30 to 75 min and in 500 mM ammonium acetate from 76 to 90 min. NO<sub>2</sub>-Cyt<sub>74</sub> and NO<sub>2</sub>-Cyt<sub>97</sub> were collected and re-purified in the same column to avoid any cross-contamination. A typical chromatogram is shown in Fig. S1. The mononitrated species (peaks B and C) were then re-purified in order to obtain pure mononitrated samples (Inset Fig S1).

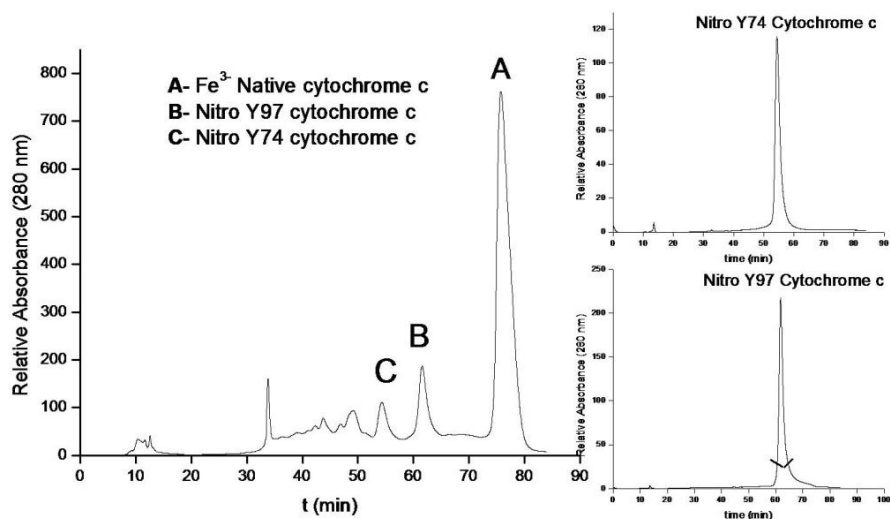


**Figure S1.** HPLC cationic exchange analysis of Cyt (3 mM) exposed to peroxynitrite. Left: Chromatogram of the mixture obtained by exposure of Cyt to peroxynitrite. Right: Re-purified nitro-Cyt species on Y74 (Upper panel) and Y97 (Lower panel).

The re-purified mono nitrated Cyt species were analyzed by MALDI-TOF MS, in order to verify the site of nitration and rule out the presence of other modifications in the sample. Nitration was confirmed by following the transition +45 Da, corresponding to the addition of a nitro group and +29 Da corresponding the to a hydroxylamine derivative that arises from the increase of 45 Da (+NO<sub>2</sub> group) minus an oxygen molecule (-16 Da) (Figure S2). This transition confirms the nitration according to previous reports.<sup>3</sup>

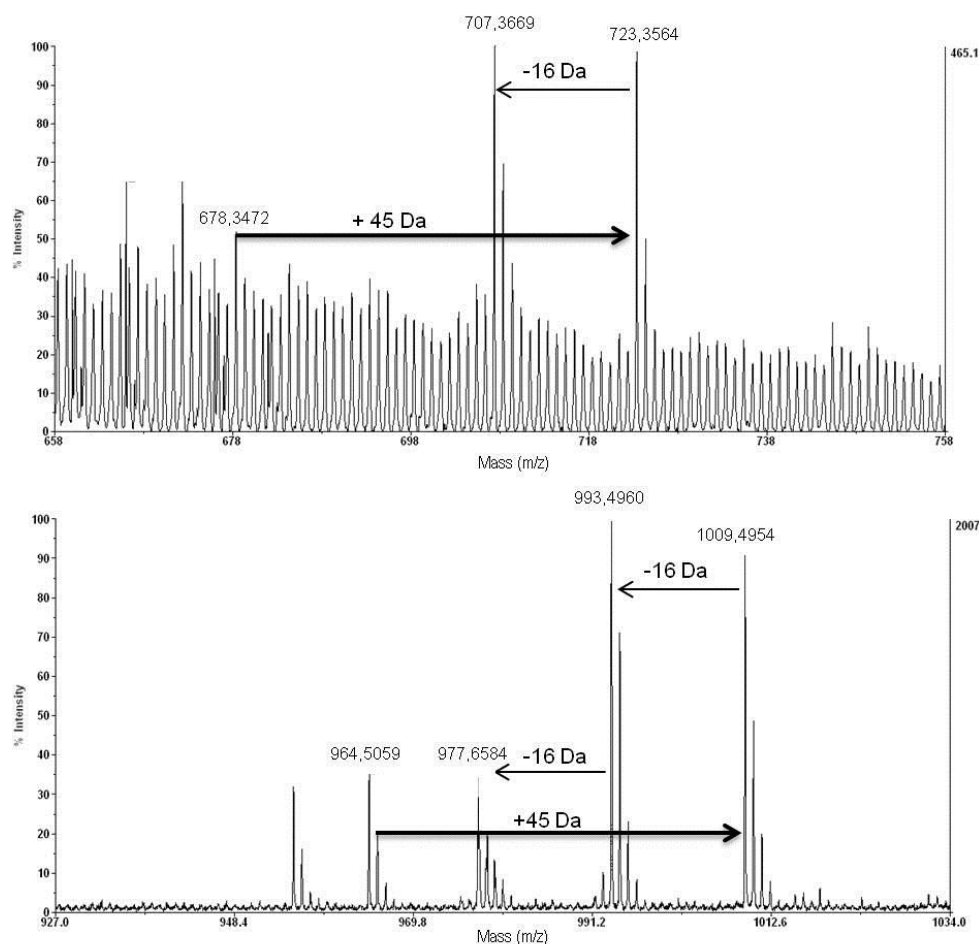


**Figure S2.** MALDI-TOF MS spectra of mono nitrated Cyt. Upper panel: Nitrated tyrosine 74 containing peptide (YIPGTK) (723 Da). Lower panel: Nitrated tyrosine 97 containing peptide (EDLIAYLK) (1009 Da).

For mass spectrometry analysis Cyt was digested with trypsin (sequence grade, Promega) as described elsewhere.<sup>4</sup> Prior to MS analyses, samples were desalted using C18 reverse phase micro-columns (Omix®Tips, Varian) and eluted directly onto the sample plate for MALDI-MS with CHCA matrix solution in aqueous 60% ACN containing 0.1% TFA. Mass spectra of peptides mixtures were acquired in a 4800 MALDI TOF/TOF instrument (Applied Biosystems) in positive ion reflector mode. Mass spectra were externally

calibrated using a mixture of peptide standards (Applied Biosystems). MS/MS analyses of selected peptides were performed. MS/MS spectra was recorded as well, confirming the site of nitration in the analyzed peptides (Table S1).

**Table S1:** Fragmentation of the peptides containing tyrosine 74 and 97. In bold are the fragments that were detected in our analysis, allowing us to confirm nitration in the residues 74 and 97 (Left and right tables, respectively).

Peptide 74-79					Peptide 94-99			
#	b	Sec	y	#	b	Sec	y	#
1	209.0557	Y		6	130.0499	E		8
2	<b>322.1397</b>	I	515.3188	5	<b>245.0768</b>	D	<b>880.4775</b>	7
3	419.1925	P	<b>402.2347</b>	4	<b>358.1609</b>	L	<b>765.4505</b>	6
4	476.2140	G	<b>305.1819</b>	3	<b>471.2449</b>	I	652.3665	5
5	<b>577.2617</b>	T	<b>248.1605</b>	2	<b>542.2821</b>	A	<b>539.2824</b>	4
6		K	147.1128	1	<b>750.3305</b>	Y	<b>468.2453</b>	3
					<b>863.4145</b>	L	<b>260.1969</b>	2
						K	<b>147.1128</b>	1

Proteins were identified by a database search of measured peptide  $m/z$  values using the MASCOT program (Matrix Science <http://www.matrixscience.com/search> form), and based on the following search parameters were considered fragment mass tolerance, 0.3 Da; partial methionine oxidation, tyrosine nitration and one missed tryptic cleavage allowed. Protein mass and taxonomy were unrestricted. Significant scores ( $p < 0.05$ ) were used as criteria for positive protein identification.

**UV-vis titrations.** Electronic absorption spectra were obtained in order to evaluate the band centered at 695 nm ( $\epsilon_{695}=865 \text{ M}^{-1} \text{ cm}^{-1}$ ), indicative of the heme iron-Met-80 coordination, using a Thermo Scientific Evolution Array spectrophotometer and a 0.5mL quartz cuvette with a 1 cm path. Assays were performed with 0.15 mM WT or 0.05mM  $\text{NO}_2\text{-Cyt}$  in 20mM HEPES buffer. The concentration of the different Cyt species was adjusted by quantitation of the Soret band absorption at 410 nm ( $\epsilon_{410}=106,000 \text{ M}^{-1} \text{ cm}^{-1}$ ). For pH titration studies, the pH of the sample was adjusted with 1M KOH prior to the addition of Cyt, and spectra were collected at each pH point.

**Resonance Raman spectroscopy.** Resonance Raman (RR) spectra were recorded either with 413 nm (3 mW, Spectra-Physics BeamLok 2060) or 458 nm excitation (8 mW, Coherent Innova 70c) in backscattering geometry using a confocal microscope coupled to a single stage spectrograph (Jobin Yvon XY 8Dop00) equipped with a CCD detector. For pH titration studies, 0.2 mM WT or  $\text{NO}_2\text{-Cyt}$  in 20mM HEPES buffer were placed into a rotating quartz cell for the measurements. Relative concentrations of the native and alkaline isomers were determined by spectral component analysis using the proportions of the two species as the only adjustable parameter, following previously described procedures and self-written software.<sup>5</sup> The titration curves shown in Figure 2 represent the RR intensity of

the  $1336\text{ cm}^{-1}$  (assigned to the  $\nu_{\text{NO}_2, \text{s}}$  mode of deprotonated Tyr)<sup>6</sup> as a function of pH, normalized by the intensity obtained at pH 10.

**Cyclic voltammetry.** Cyclic voltammetry (CV) experiments in solution were performed with a Gamry REF600 potentiostat using a non-isothermal cell equipped with a polycrystalline gold bead working electrode, a Pt wire auxiliary electrode and a Ag/AgCl (3.5 M KCl) reference electrode to which all potentials in this work are referred. Au electrodes were first oxidized in 10% HClO<sub>4</sub> applying a 3 V potential for 2 min, sonicated in 10% HCl for 15 min, rinsed with water and subsequently treated with a 3:1 v/v H<sub>2</sub>O<sub>2</sub>:H<sub>2</sub>SO<sub>4</sub> mixture at 120 °C. The electrodes were then subjected to repetitive voltammetric cycles between -0.2 and 1.6 V in 10% HClO<sub>4</sub> and thoroughly washed with water and ethanol. Au working electrodes were coated with self-assembled monolayers (SAMs) by overnight incubation in a 0.2 mM solution the alkanethiol HS-(CH<sub>2</sub>)<sub>5</sub>-CH<sub>2</sub>OH. CV determinations were performed in a 0.2 mM solution of Cyt in HEPES buffer 20 mM.

**Molecular dynamics simulations.** The starting structure for simulations of Cyt in the ferric state corresponds to the oxidized form of WT horse heart Cyt (PDB ID 1HRC). All structures were minimized in a TIP3P water box and then heated and equilibrated at 300K using standard procedures.<sup>7</sup> All systems were simulated at 300 K and 1 bar, maintained with the Berendsen thermostat and barostat respectively, employing periodic boundary conditions and Ewald sums for treating long-range electrostatic interactions.

NO<sub>2</sub>-Cyt<sub>74</sub> was built *in silico* replacing the corresponding side chains and relaxing the resulting structure using classical MD. Partial charges for the protonated and deprotonated nitro-tyrosine were obtained from RESP calculations computed using Hartree-Fock with a 6-31G/basis set.<sup>8</sup>

Production runs of 50 ns were obtained for WT, NO<sub>2</sub>-Cyt<sub>74</sub> and deprotonated NO<sub>2</sub>-Cyt<sub>74</sub>.

To obtain thermodynamic information of the Fe-Met80 dissociation process, free energy profiles were computed. The profiles were constructed by performing constant velocity steered molecular dynamics (SMD) simulations and using Jarzynski's equality, which relates equilibrium free energy ( $\Delta G$ ) values with the irreversible work performed over the system. The reaction coordinate was chosen as the Fe(heme)-S(Met80) distance.

*In silico* models for alkaline Cyt were obtained starting from the NMR structure of alkaline iso-Cyt in which the sixth axial ligand is Lys73 (PDB ID 1LMS). This structure was reported by Assfalg et al.<sup>9</sup> from yeast iso-1-ferricytochrome *c* triple variant (Lys72Ala/Lys79Ala/Cys102Thr) in an alkaline conformation. Our model for alkaline Cyt is a chimeric structure in which the conformation of the  $\Omega$  loop consisting of residues 70-88 of 1HRC was replaced by that of 1LMS, while retaining the aminoacidic sequence of the horse heart variant.

After equilibration, production runs of 10 ns were obtained for the alkaline isomer of WT, NO<sub>2</sub>-Cyt<sub>74</sub> and deprotonated NO<sub>2</sub>-Cyt<sub>74</sub>. Analogous SMD simulations were performed for these structures. In these cases, the reaction coordinate was chosen as the Fe(heme)-N(Lys73) distance.

#### ***Peroxidatic activity determinations.***

Assessment of peroxidase activity with Amplex UltraRed Reagent (purchased from Invitrogen) was performed using the fluorescence of resorufin, an oxidation product of Amplex Red ( $\lambda_{\text{ex}} = 570\text{ nm}$ ,  $\lambda_{\text{em}} = 585\text{ nm}$ ). Briefly, 0.5  $\mu\text{M}$  Cyt was incubated in HEPES

(10 mM plus 100  $\mu$ M DTPA), pH 7. Then, 50  $\mu$ M Amplex Red and 25  $\mu$ M  $H_2O_2$  were added in HEPES (100 mM plus 100  $\mu$ M DTPA) at different pHs and the fluorescence was registered using a FLUOstar Optima plate fluorimeter (BMG Labtech). The reaction rate was determined by linear fit of the fluorescence intensity. Results are summarized in Table S2.

**Table S2:** Peroxidatic activity of nitrated Cyt species.

	Peroxidatic activity at pH 5		Peroxidatic activity at pH 7		Peroxidatic activity at pH 9	
	$\mu$ M/min	% of control	$\mu$ M/sec	% of control	$\mu$ M/sec	% of control
WT	$4.5 \pm 0.5$	100	$1.7 \pm 0.1^a$	100	$0.13 \pm 0.01$	100
$NO_2$ -Cyt <sub>74</sub>	$17 \pm 5$	367	$9.3 \pm 1.7$	547	$0.89 \pm 0.15$	768
$NO_2$ -Cyt <sub>97</sub>	$8 \pm 1$	169	$3.8 \pm 0.7$	221	$0.21 \pm 0.03$	161

<sup>a</sup>According to Souza et al.<sup>2</sup>

### Additional supplementary figures.

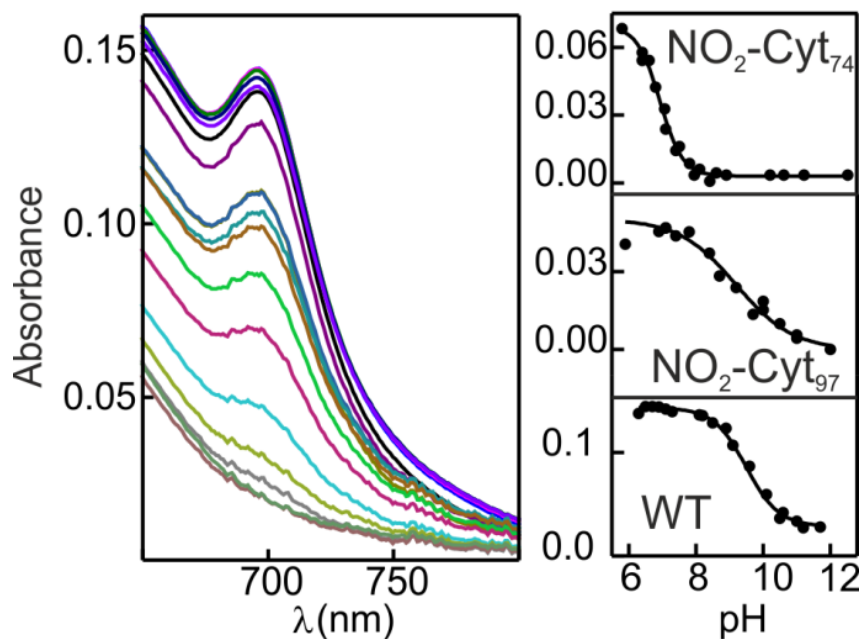


**Figure S3.** Equilibrium alkaline transition of non-nitrated and nitrated Cyt monitored by UV-vis absorption. Left: absorption spectra of WT as a function of pH. Right: absorbance at 695 nm as a function of pH for  $NO_2$ -Cyt<sub>74</sub>,  $NO_2$ -Cyt<sub>97</sub> and WT.

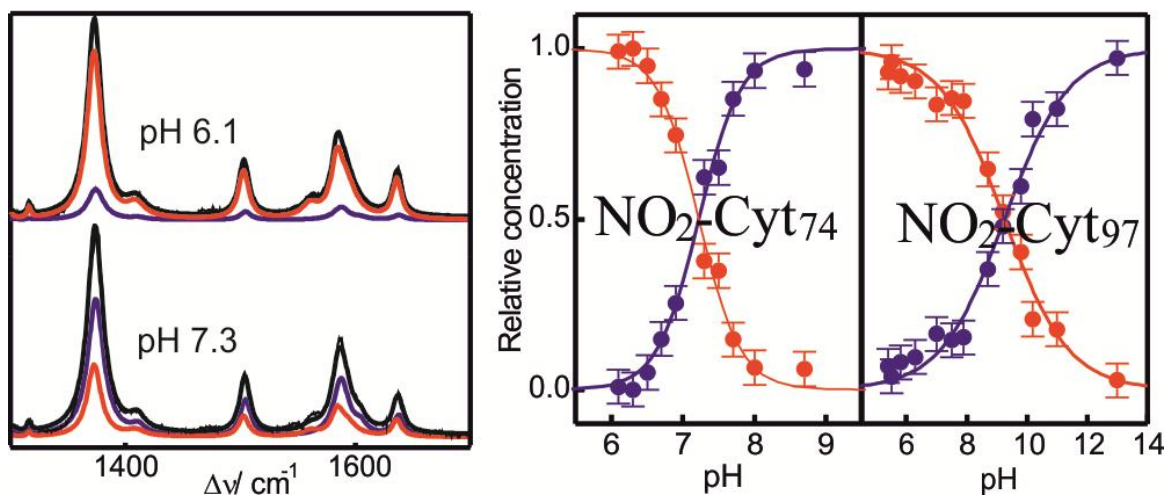


**Figure S4.** Left: RR spectra of ferric NO<sub>2</sub>-Cyt74 recorded at different pH values ( $\lambda_{\text{ex}} = 413$  nm). Black: experimental spectra. Red: native spectral component. Blue: alkaline spectral component. Right: Relative concentrations of the native (red) and alkaline (blue) isomers of NO<sub>2</sub>-Cyt74 and NO<sub>2</sub>-Cyt97 as a function of pH, as determined by RR.

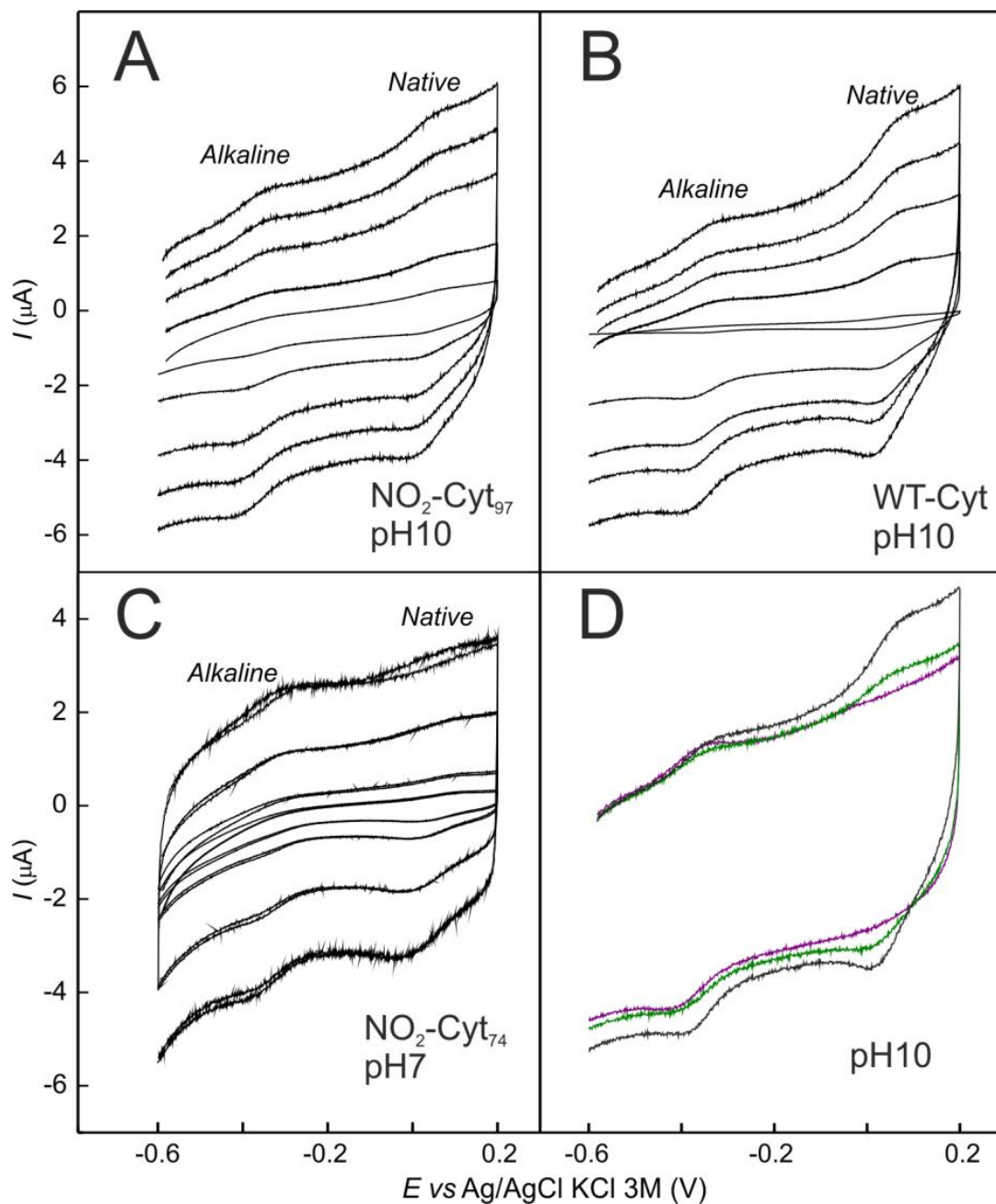


**Figure S4.** Cyclic voltammograms obtained in solution at different scan rates between 0.01 and 10  $\text{V s}^{-1}$  for: (A)  $\text{NO}_2\text{-Cyt}_{97}$  in 20 mM HEPES, pH 10; (B) WT Cyt in 20 mM HEPES, pH 10; (C)  $\text{NO}_2\text{-Cyt}_{74}$  in 20 mM HEPES, pH 7, (D) WT-Cyt (black),  $\text{NO}_2\text{-Cyt}_{97}$  (green) and  $\text{NO}_2\text{-Cyt}_{74}$  (purple) in 20 mM HEPES pH 10. The protein concentration was 0.2 mM in all cases.

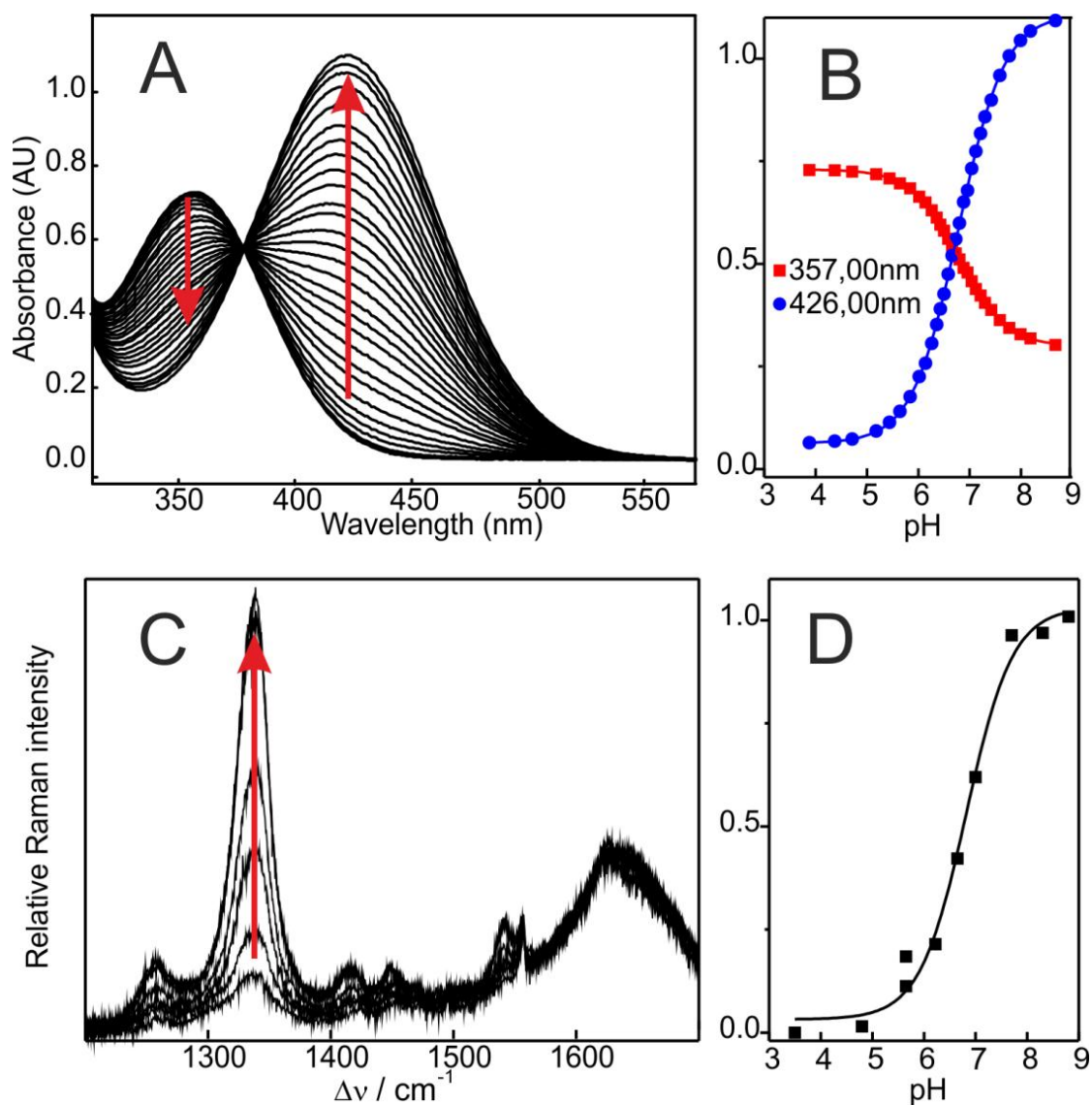


**Figure S6.** Acid-base titration of free 3-NO<sub>2</sub>-Tyr in solution monitored by UV-vis absorption (A and B) and by resonance Raman spectroscopy under 458 nm excitation (bottom). The arrows indicate increasing pH.

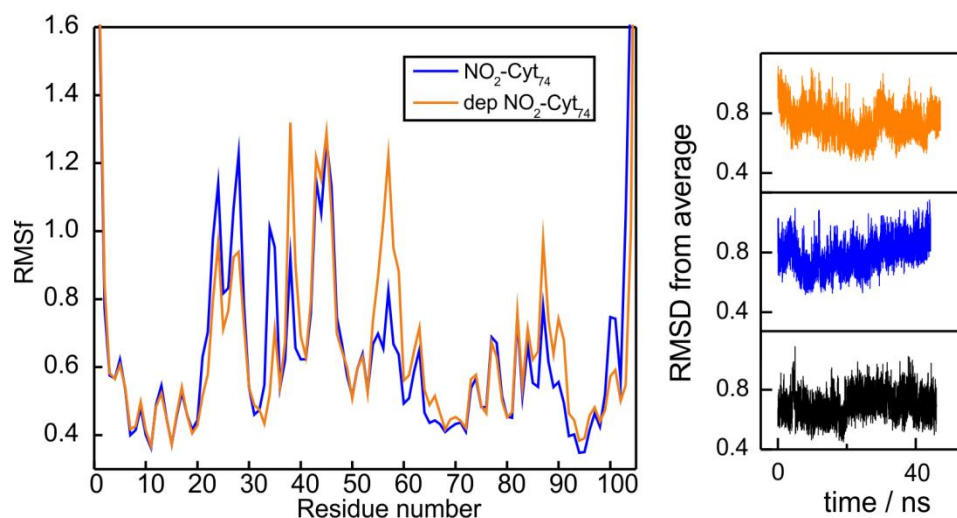


**Figure S7.** Results from MD simulations. Left: Per residue root mean square fluctuations (RMSf) for the native conformation (Met/His) of protonated (blue) and deprotonated (orange) NO<sub>2</sub>-Cyt<sub>74</sub>, with respect to WT-Cyt. Right: Root mean square deviations (RMSD) with respect to average as a function of the simulation time for the native conformers (Met/His) of WT-Cyt (black), protonated NO<sub>2</sub>-Cyt<sub>74</sub> (blue) and deprotonated NO<sub>2</sub>-Cyt<sub>74</sub> (orange). The time step is 2ps for all simulations.

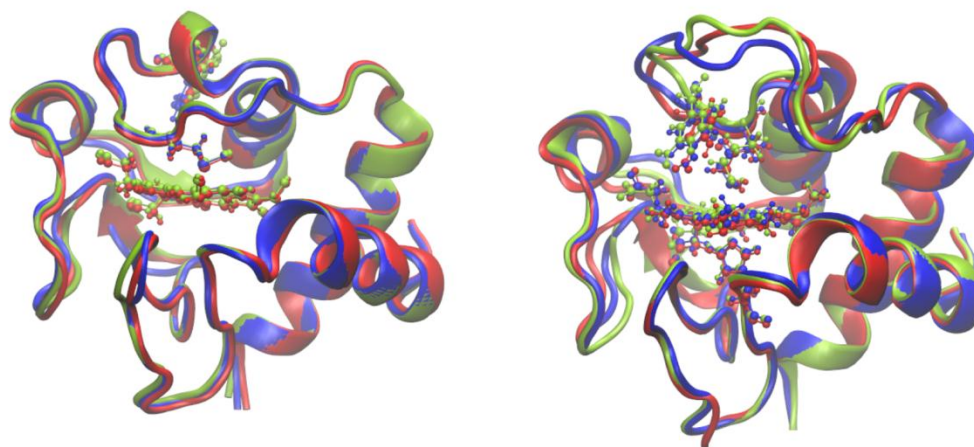


**Figure S8.** Left: Structural comparison of the native isomers (Met/His) of WT-Cyt (blue) with the protonated (red) and deprotonated (green) forms of NO<sub>2</sub>-Cyt<sub>74</sub>. Right: Structural comparison of the alkaline isomers (Lys/His) of non-nitrated Cyt (blue) with the protonated (red) and deprotonated (green) forms of NO<sub>2</sub>-Cyt<sub>74</sub>.

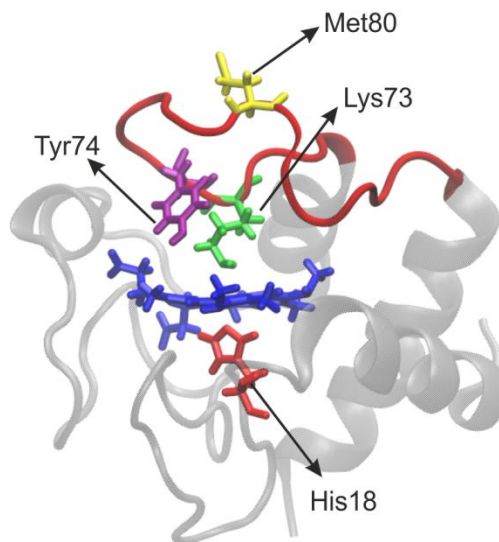


**Figure S9.** *In silico* generated model structure of the alkaline isomer of Cyt. Red ribbon:  $\Omega$ -loop consisting of residues 70-88 adopted from the structure PDB ID 1LMS. Blue: Heme. Yellow: Methionine 80. Purple: Tyrosine 74. Green: Lysine 73. Red: Histidine 18.

## References

1. C. Batthyány, J. M. Souza, R. Durán, A. Cassina, C. Cerveñansky, and R. Radi, *Biochemistry*, 2005, **44**, 8038–46.
2. J. M. Souza, L. Castro, A. M. Cassina, C. Batthyány, and R. Radi, *Methods Enzymol.*, 2008, 441, 197–215.
3. A. Sarver and N. Scheffler, *J. Am. Soc. Mass Spectr.*, 2001, **305**, 439–448.
4. U. Hellman in *Proteomics in Functional Genomics*, P. Jollès and Jörnvall Eds., Birkhäuser Verlag, Basel, Jörnvall E., 2000.
5. S. Döpner, P. Hildebrandt, H. Lenk, W. Stempfle, and A. G. Mauk, *Spectrochim. Acta A*, 1996, **51**, 573–584.
6. L. Quaroni and W. Smith, *J. Raman Spectr.*, 1999, **542**, 537–542.
7. D. Alvarez-Paggi, M. a Castro, V. Tórtora, L. Castro, R. Radi, and D. H. Murgida, *J. Am. Chem. Soc.*, 2013, **135**, 4389–97.
8. D. M. Moreno, M. A. Martí, P. M. D. Biase, D. A. Estrin, V. Demicheli, R. Radi, and L. Boechi, *Arch. Biochem. Biophys.*, 2011, **507**, 304–309.
9. M. Assfalg, I. Bertini, A. Dolfi, P. Turano, a G. Mauk, F. I. Rosell, and H. B. Gray, *J. Am. Chem. Soc.*, 2003, **125**, 2913–22.